Progress In Electromagnetics Research C, Vol. 95, 75–89, 2019

Three-Dimensional Magnetic and Temperature Field Coupling Analysis of Dry-Type Transformer Core under Different Excitations

Yongqiang Wang*, Zhaoxin Wang, and Sen Fang

Abstract—To study the transient magnetic field and temperature field of a dry-type transformer core and analyze the core loss and hot spot temperature rise of the core, a magnetic and temperature field coupling analysis method based on finite element method was proposed: the transient magnetic field of dry-type transformer was calculated first, and the core loss under a no-load condition was obtained. Then, the core loss density distribution was coupled to the temperature field as the heat source, and the temperature field distribution in the transformer was calculated by the fluid-thermal coupling method to obtain the hot spot temperature and the position of the core. Compared with the traditional average heat source method, the temperature field distribution calculated by the proposed method is close to the actual temperature distribution of the core. Finally, based on this method, the magnetic field and temperature field of the transformer core under different excitations were calculated, and the effect of harmonics on the core loss and temperature rise of the core was analyzed.

1. INTRODUCTION

Power transformers are the most vital and costly investment in a power system. The effect of its loss on the economic operation of the system cannot be ignored [1]. Nowadays, dry-type transformers are increasingly used as distribution transformers due to their superior environmental performance, strong short-circuit resistance, and low onerous maintenance requirements. Under different conditions including harmonics, a temperature of transformer will rise abnormally, and the loss therefrom will increase, which will lead to insulation deterioration and a significantly shortened service life, and finally affect its safe and stable operation [2, 3]. Therefore, studying the magnetic field distribution and loss of dry-type transformers under different conditions and obtaining their temperature field distribution are of great value to the design, manufacture, fault detection, and safe, stable operation of dry-type transformers [4].

Traditional analytical method cannot reflect the temperature field distribution on a transformer, so scholars currently use the finite element method (FEM) to analyze the magnetic field and temperature field [5, 6]. At present, the research on the transformer under different conditions mainly focuses on winding, but the core loss caused by the harmonic cannot be ignored [7]. The reduction in distribution transformer no-load losses has become a priority issue. No-load loss is sensitive to the distortion of the supply voltage waveform [8]; therefore, it is necessary to study the transient magnetic field of the transformer before analyzing the core loss and temperature rise of the core under harmonic conditions.

In the analysis of transformer temperature field, the traditional method of average heat source analysis is usually adopted [9, 10], but the influence of the distribution of core loss density cannot be considered on the temperature field of the transformer.

Scholars have conducted some research on magneto-thermal coupling of the transformer. A simple two-dimensional (2-d) model was adopted to analyze the magnetic field and temperature field of the

Received 4 July 2019, Accepted 10 August 2019, Scheduled 26 August 2019
* Corresponding author: Yongqiang Wang (qianghd@126.com).
The authors are with the School of North China Electric Power University, Baoding 071003, China.

transformer by FEM [11, 12]. A three-dimensional (3d) magneto-thermal coupling analysis model of the transformer was established [13–15]. However, they did not consider the effect of air flow velocity instead of using heat transfer coefficient to analyze the temperature field. In general, the value of heat transfer coefficient is a complicated function of the fluid flow, the thermal properties of the fluid medium, and the geometry of the system. Such a broad dependence makes it difficult to obtain an analytical expression for the heat transfer coefficient [16]. Scholars have investigated temperature fields while considering the effect of air flow velocity. A 2-d fluid-thermal coupled model was introduced to investigate the thermal performance of an oil-immersed transformer [16]. An advanced 3-d FEM model for the coupled solution of heat transfer and fluid flow was presented in [17].

In view of the above problems, an improved 3-d magnetic and temperature field coupling analysis method of a dry-type transformer based on FEM considering the effect of air flow velocity was proposed in this paper. The transient magnetic field of the dry transformer was analyzed based on FEM, and the magnetic field and loss density distribution of the core were obtained. Based on the results of magnetic field analysis, the loss density distribution of the core was applied to the temperature field as the heat source. Meanwhile, considering the air flow field, the fluid-thermal coupling method was adopted to analyze the temperature field distribution of the temperature. Then, the influence of different excitations including harmonics on core loss and temperature rise of a dry transformer core was analyzed.

2. THEORETICAL ANALYSIS OF MAGNETIC AND TEMPERATURE FIELDS OF DRY-TYPE TRANSFORMER

2.1. Core Loss and Magnetic Field Analysis of Dry-Type Transformer

When a dry-type transformer is in its normal mode of operation, losses will occur on the core, windings, and other structural components under the action of the magnetic field. These losses are converted into heat, causing the temperature of the transformer to rise. Transformer losses mainly include copper loss and core loss. Copper loss is caused by the current passing through the winding. We mainly studied the core loss of the transformer, which can be decomposed into eddy current loss and hysteresis loss. The expression of core loss under rated conditions is [18]:

$$P_{Fe} = p_h + p_e = K_c f B_m^{1.6} + K_e f^2 B_m^2 \Delta^2 \tag{1}$$

where P_{Fe} represents the rated core loss, K_c the hysteresis loss coefficient, K_e the eddy current loss coefficient, f the rated frequency, B_m the maximum magnetic flux density, and Δ the thickness of the silicon steel sheet.

The expression of the core loss $P_{Fe(l)}$ generated by the l^{th} harmonic is:

$$P_{Fe(l)} = p_{h(l)} + p_{Fe(l)} = l k_{Bm(l)}^{1.6} p_h + l^2 k_{Bm(l)}^2 p_e \tag{2}$$

where $k_{Bm(l)} = \frac{B_{m(l)}}{B_{m(1)}}$ is the maximum magnetic flux density ratio of the l^{th} harmonic.

Most transformer cores are made of stacking silicon steel sheets with high resistivity to reduce eddy current loss. Under rated conditions, the eddy current loss accounts for about 50% of the core loss; therefore $p_h \approx p_e$. The l^{th} harmonic maximum magnetic flux density ratio is equal to the l^{th} harmonic magnetic flux density ratio, $k_{Bm(l)} = k_{B(l)}$. It can be seen that:

$$P_{Fe(l)} = P_{Fe} \cdot \frac{(l k_{Bm(l)}^{1.6} + l^2 k_{Bm(l)}^2)}{2} = P_{Fe} \cdot \frac{(l^{-0.6} k_{e(l)}^{1.6} + l k_{e(l)}^2)}{2} \tag{3}$$

where $k_{B(l)}$ is the l^{th} harmonic magnetic flux density ratio, and $k_{e(l)}$ is the harmonic voltage ratio:

$$k_{B(l)} = \frac{B_{(l)}}{B_{(1)}} \times 100\% \; k_{e(l)} = \frac{U_{(h)}}{U_{(1)}} \times 100\% \tag{4}$$

where $B_{(l)}$ is the l^{th} harmonic magnetic flux density; $B_{(1)}$ is the fundamental magnetic flux density; $U_{(h)}$ and $U_{(1)}$ are the root mean square (rms) l^{th} harmonic voltage and the rms fundamental voltage, respectively.

It can be seen from the above equation that the no-load loss of the transformer under harmonic excitation is related to the harmonic voltage ratio and harmonic order.

The magnitude of core loss is related to the distribution of magnetic flux density of the core, so it is necessary to analyze the magnetic field of the transformer before calculating the core loss. The governing equation based on the magnetic vector potential A is:

$$\nabla \times \frac{1}{\mu}(\nabla \times A) = J_s - \sigma \frac{\partial A}{\partial t} \tag{5}$$

where μ denotes the permeability, σ the conductivity, and J_s the current density of the winding.

The unit magnetic flux density can be calculated after obtaining the magnetic vector potential A, and the loss of each unit of the core can be obtained from the B-P curve corresponding to the unit mass loss.

2.2. Heat Transfer and Temperature Field Analysis of Dry-Type Transformer

The heat generated by the core and windings in the transformer is transmitted in three ways: heat conduction, heat convection, and heat radiation. Heat conduction occurs mainly in the solid region such as the core and windings of the transformer. Heat convection mainly occurs in the fluid region, and heat is carried away by the flow of air. Heat radiation occurs mainly between components at different temperatures. With constant heat generation and heat dissipation, the temperature of the transformer finally reaches a dynamic equilibrium.

The governing equation of fluid-thermal field in dry-type transformer is as follows: Equation (6) is the mass conservation equation, also known as continuity equation; Equation (7) is the momentum conservation equation; Equation (8) is the energy conservation equation:

$$\nabla \cdot U = 0 \tag{6}$$

$$(\rho U \cdot \nabla) + \nabla p - \mu_0 \nabla^2 U = f \tag{7}$$

$$\nabla \cdot (\rho c_p U T) - \nabla \cdot \lambda \nabla T = S_T \tag{8}$$

where U is the velocity vector of air; p is the fluid pressure; f is the external force density vector; ρ is the density of the fluid; μ_0 is the dynamic viscosity coefficient; c_p is the specific heat capacity; T is the scalar value of the transformer temperature; λ is the coefficient of thermal conductivity; S_T is the amount of heat source.

The heat transfer problem in solid regions can be solved by the heat transfer equation, while the fluid heat transfer problem is relatively complex. Air flow and heat transfer problems can be solved by use of the mass conservation equation, momentum conservation equation, and energy conservation equation. Among them, the mass conservation equation and momentum conservation equation can be used to calculate the fluid and velocity distribution. The energy conservation equation can be used to calculate the temperature distribution of the fluid domain. The final flow velocity and temperature of the field can be calculated by coupling the flow field and temperature field equations.

3. MAGNETIC AND TEMPERATURE FIELD COUPLING ANALYSIS OF DRY-TYPE TRANSFORMER CORE UNDER POWER FREQUENCY BASED ON FEM

3.1. CALCULATION MODEL

FEM software ANSYS 18.0 was used to analyze the magnetic field and temperature field of the dry-type transformer. ANSYS software combines the electromagnetic field calculation module Maxwell and the temperature field calculation module Fluent.

3.1.1. Assumptions

The transient magnetic field distribution and core loss density distribution of the core were obtained by using Maxwell to analyze the transient magnetic field of the transformer. Then the loss distribution is coupled to Fluent as the heat source, and the temperature distribution of the core under corresponding loss distribution is simulated based on the fluid-thermal coupling temperature field analysis method.

To simplify the calculation, the following assumptions are made:

(1) The distribution of magnetic field and temperature field of the core was mainly studied, so windings were simplified as a ring concentric with the core column.

(2) Only the air, core, and windings were considered, while the clamp frame, compressing plate, magnetic shield, and copper shield were not considered.

(3) The ambient temperature was 20°C.

3.1.2. Physical Model and Physical Parameters

A cast-resin dry-type transformer is taken as an example. The main parameters of the transformer are shown in Table 1. Based on the actual size of the transformer, the physical model of the dry-type transformer was established (Figure 1). The physical properties of the transformer materials are listed in Table 2. The specific type of silicon steel sheet used by the transformer core is DW310-35, and the B-H curve and B-P curve at different frequencies are shown in Figure 2 and Figure 3.

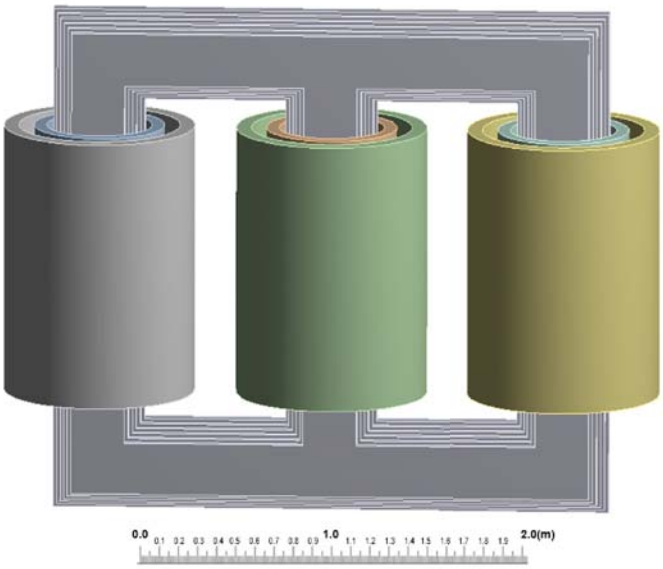

Figure 1. Physical model of the dry-type transformer.

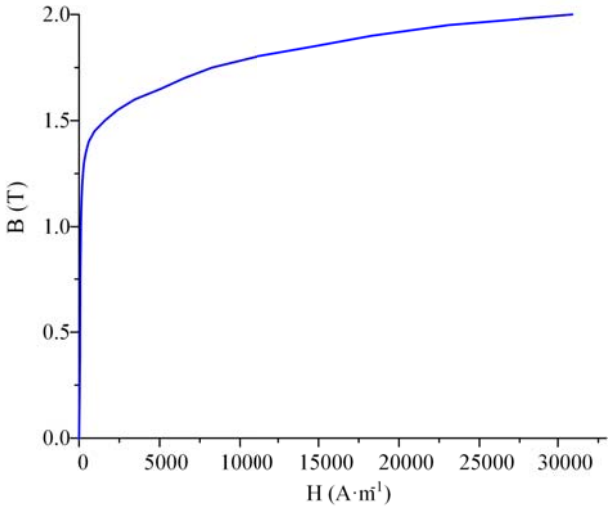

Figure 2. B-H curve.

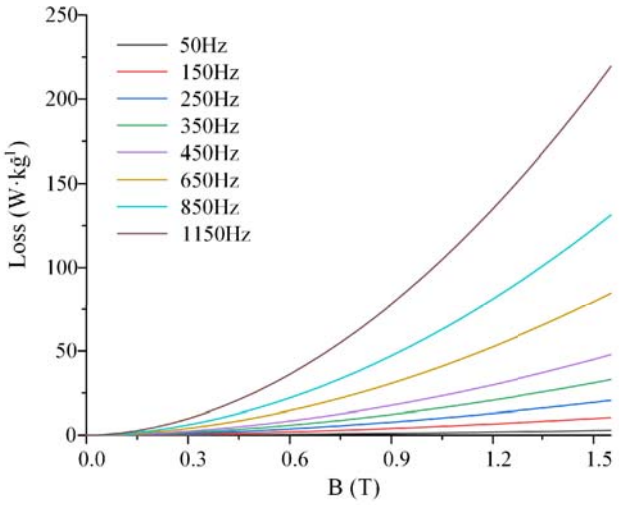

Figure 3. B-P curve at different frequencies.

Table 1. Main parameters of the transformer.

Rated power/kW	Frequency/Hz	Rated voltage/kV	No-load loss/W	Load Loss/W
10000	50	35/6.3	9840	37820

Table 2. Physical parameters of transformer materials.

Material	Parameters	Value/Formula
core	density/$\mathrm{kg}\cdot\mathrm{m}^{-3}$	8900
	coefficient of thermal conductivity/$\mathrm{W}\cdot(\mathrm{m}\cdot\mathrm{K})^{-1}$	390
	Specific heat capacity/$\mathrm{J}\cdot(\mathrm{kg}\cdot\mathrm{K})^{-1}$	338
	Relative permeability	B-H curve
wingding	density/$\mathrm{kg}\cdot\mathrm{m}^{-3}$	7650
	coefficient of thermal conductivity/$\mathrm{W}\cdot(\mathrm{m}\cdot\mathrm{K})^{-1}$	460
	Specific heat capacity/$\mathrm{J}\cdot(\mathrm{kg}\cdot\mathrm{K})^{-1}$	45
air [9]	density/$\mathrm{kg}\cdot\mathrm{m}^{-3}$	$\rho = 1.263e^{-0.003T}$
	coefficient of thermal conductivity/$\mathrm{W}\cdot(\mathrm{m}\cdot\mathrm{K})^{-1}$	$v = 1.755e^{-5} + T \times 4.1e^{-8}$
	Specific heat capacity/$\mathrm{J}\cdot(\mathrm{kg}\cdot\mathrm{K})^{-1}$	$\lambda = 0.0237 - T \times 7e^{-5}$
	Dynamic viscosity/$\mathrm{kg}\cdot(\mathrm{m}\cdot\mathrm{K})^{-1}$	$c_P = 1.011 + 1.103 \times T$

3.1.3. Mesh

Before simulating, it is necessary to mesh the physical model of the transformer. The result of mesh is shown in Figure 4. Figure 4(a) shows the mesh of the core and windings; Figure 4(b) shows the mesh of transformer section. The tetrahedral mesh is used for domain division, and a hexahedral mesh is adopted for regular winding shape modelling, which ensures accuracy and takes the calculation time into consideration. The size of the core grid is no more than 20 mm, the size of the winding grid no more than 35 mm, and the size of the air grid no more than 50 mm.

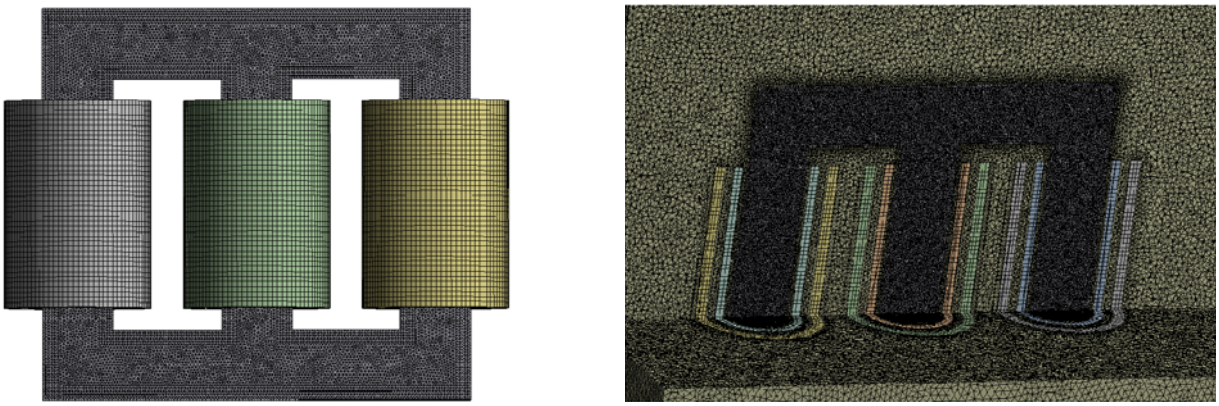

(a) (b)

Figure 4. Mesh results.

3.1.4. Boundary Condition

At the fluid-solid coupling interface, the fluid near the wall is stagnant and in a non-slip state, and it can be approximately considered that the fluid layer near the wall surface is stationary relative to the wall

surface. The heat transfer is mainly through thermal convection and thermal radiation, but thermal radiation has little impact on the heat transfer process of dry-type transformer, which can be ignored compared with the influence of thermal convection on the thermal process. The boundary condition is

$$q = -\lambda_S \frac{\partial T_S}{\partial x}\bigg|_{x=0} = -\lambda_L \frac{\partial T_L}{\partial x}\bigg|_{x=0} \tag{9}$$

In the formula, λ_S is the thermal conductivity of the solid; λ_L is the thermal conductivity of air; T_S and T_L are respectively the solid temperature and fluid temperature at the interface of fluid-solid coupling. x is the distance between the fluid-solid coupling interface and the mesh points of the adjacent layer.

In the simulation analysis of temperature field, the fluid temperature gradient at the interface of fluid and solid of the transformer is obtained by the temperature difference between the interface and the mesh points of the adjacent layer. Therefore, in the process of meshing, the mesh at the interface is relatively fine.

3.2. Transient Magnetic Field Analysis and Core Loss Calculation of a Dry-Type Transformer Core

The transient magnetic field of the dry-type transformer was calculated under no-load condition, with excitation caused by applying its rated voltage to the primary winding (with the secondary winding left open), and the transient magnetic analysis result could be obtained. The magnetic flux density distribution of the core at the peak time of each phase is shown in Figure 5.

Figures 5(a)–5(f) are transient magnetic field distribution and magnetic flux density vector distribution of the core at the peak time of phases A, B, and C of the high voltage winding, respectively. When the alternating voltage is applied to the high voltage winding, the alternating current flows through the high voltage winding and creates the alternating flux in the core that varies with time. At the peak time of phase A high-voltage winding, the voltage of phase A winding is the highest; the magnetic flux of phase A core column is the largest; a closed loop of the magnetic flux is formed through phase B and phase C core columns. Therefore, the magnetic flux density of phase B and C core column is about half that of phase A, and the maximum flux density of the core appears on the core column of phase A high voltage winding. Similarly, Figures 5(c)–5(f) are the magnetic flux density distribution of the core at the peak time of phase B and phase C high voltage winding. The maximum flux density for phase A of the core is 1.56 T, for phase B is 1.51 T, and for phase C is 1.56 T.

The main flux is closed along the core, and the leakage flux is closed along the non-ferromagnetic material (air). Since the core is made of silicon steel sheets with high magnetic conductivity, its magnetic conductivity is much larger than that of air. Therefore, the main magnetic flux accounts for most of the total magnetic flux while the leakage magnetic flux only accounts for a small part under no-load operation; thus, the magnetic flux density at the end of core columns is relatively small, and the minimum flux density appears at the outer corner of the core. Since the applied voltage is sinusoidal wave, the electromotive force and the main flux balanced with it are also sinusoidal waves. However, due to the saturation of the core, the no-load current is distorted, which will affect the waveform of main flux and phase electromotive force. Therefore, the magnetic flux densities of the other two phases of the core column are not completely symmetric when the winding peaks in one phase.

Figure 6 shows the core loss density distribution of the dry-type transformer. It can be seen that the core loss distribution of the transformer has similar characteristics to the magnetic flux density distribution. The loss densities at the outer corner of the core and the upper and lower sides of the core column are small. The average loss of the core is the largest in the B-phase column. By integrating the loss density of the core, the total core loss at the power frequency was obtained (9319.2 W here). As shown in Table 3, the no-load loss of the transformer provided by the manufacturer was compared with the simulated value. The deviation between the simulated value and experimental value is less than 15%, which indicates that the magnetic field analysis of the transformer is correct and lays a foundation for the study of the magnetic-temperature field coupling analysis of the transformer.

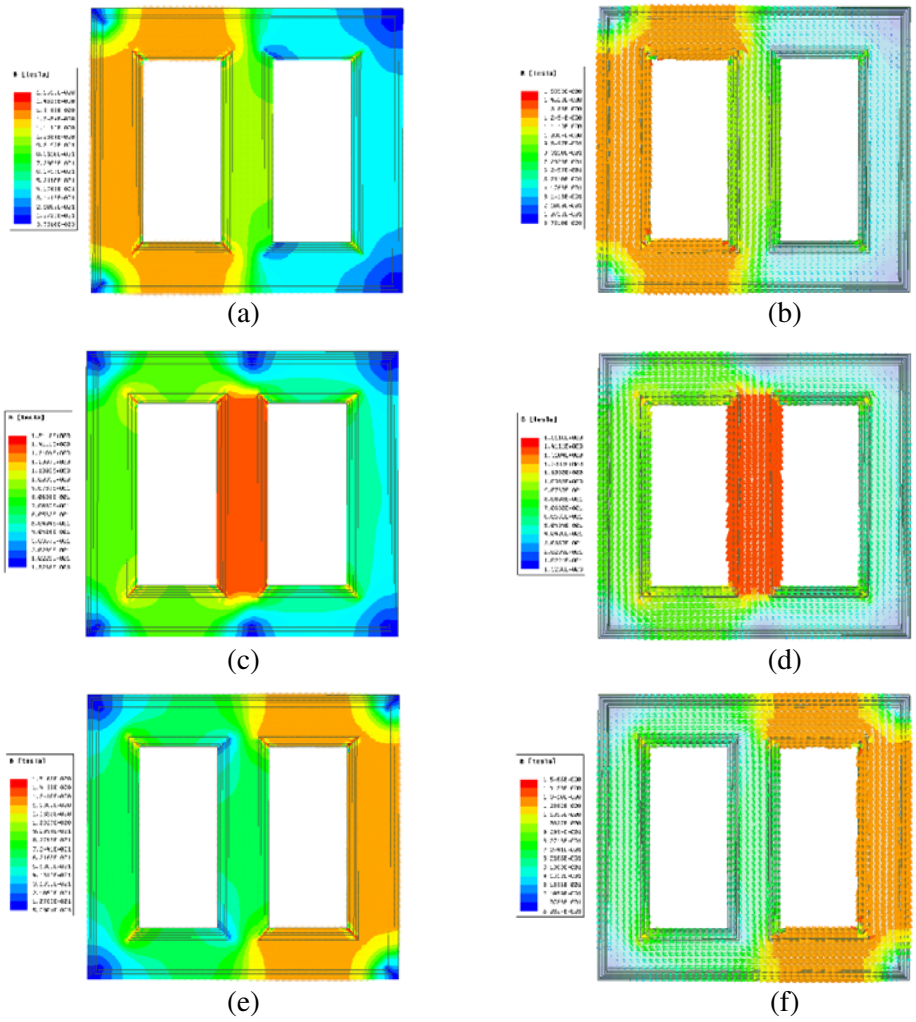

Figure 5. Magnetic flux density distribution of a dry-type transformer core.

Table 3. Comparison of simulated and experimental values of core loss at the power frequency.

experimental value	simulated value	deviation
9840 W	9319.2 W	5.29%

3.3. Temperature Field Analysis of Dry-Type Transformer Based on Core Loss Density Distribution

The loss distribution results were loaded onto the transformer core as a heat source, and the temperature distributions of the core under no-load and load conditions were calculated. Meanwhile, the traditional average heat source method was used to simulate the temperature field of the dry-type transformer core, and the calculated results were compared and analyzed.

3.3.1. Analysis of Temperature Field of the Core Under No-Load Condition

The temperature field distribution of the core obtained by the magnetic field and temperature field coupling method is shown in Figure 7. Figure 7(a) shows the temperature field distribution nephogram of the core, and Figure 7(b) shows the axial temperature distribution curve of the core.

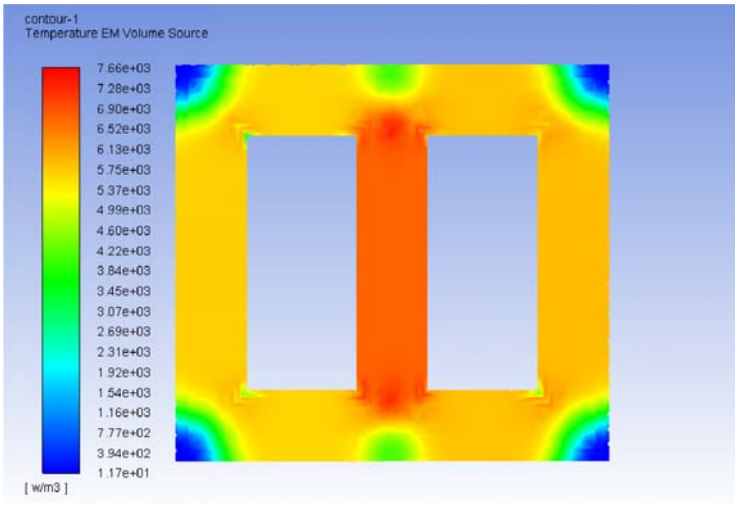

Figure 6. Core loss density distribution of the dry-type transformer.

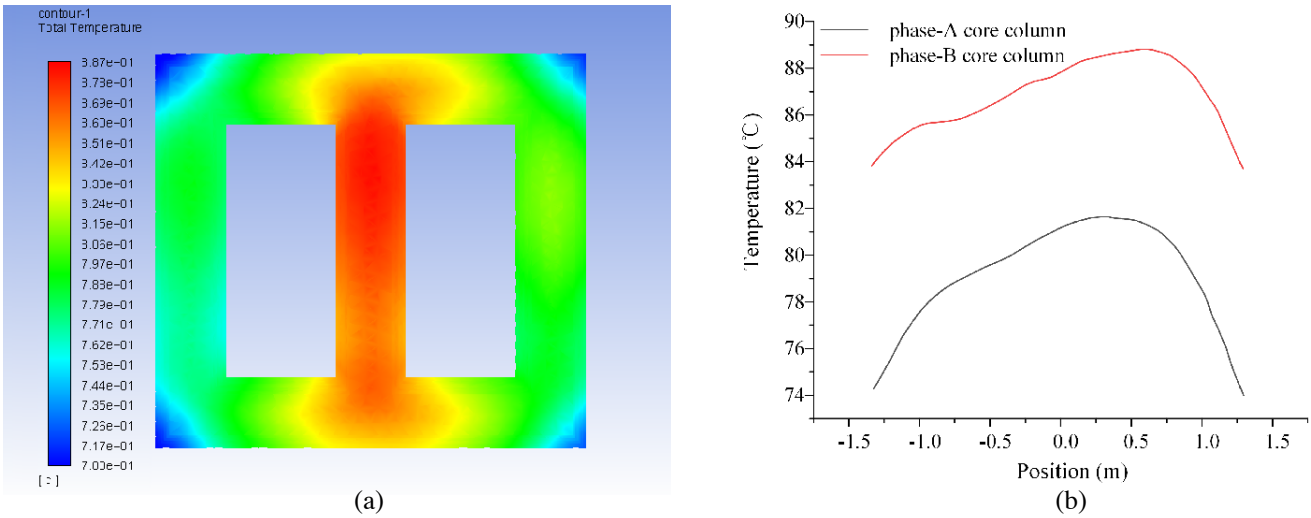

Figure 7. Temperature field distribution of a dry-type transformer core under no-load condition.

Under no-load condition, the hot spot temperature of the core is 88.7°C, and the temperature rise is 68.7°C. The position of the hot spot of the core is located near the upper end of the middle core column, which is consistent with the actual situation. As can be seen from Figure 7(b), the temperature of the core first increases and then decreases, along the axis, and the temperature at both ends is lower. This is because the heat dissipation conditions at the end of the core volume are better than in the middle. The temperature of the B-phase column of the core is high, because phase A and phase C core columns have more heat dissipation area in contact with the air, and the cooling media on both sides have a better circulatory path, so the heat dissipation effect is enhanced. Besides, the heat source is slightly larger than that in the other two phases. The temperature at the four corners of the core is significantly lower than the temperature of the core column, because the loss densities at the four corners of the core are smaller than the loss densities in other regions, and thus the rate of heat generation is lower.

3.3.2. Analysis of Temperature Field of the Core Under Load

The temperature field distribution of the core under load is shown in Figure 8: Figure 8(a) shows the temperature field distribution nephogram of the core, and Figure 8(b) shows the axial temperature

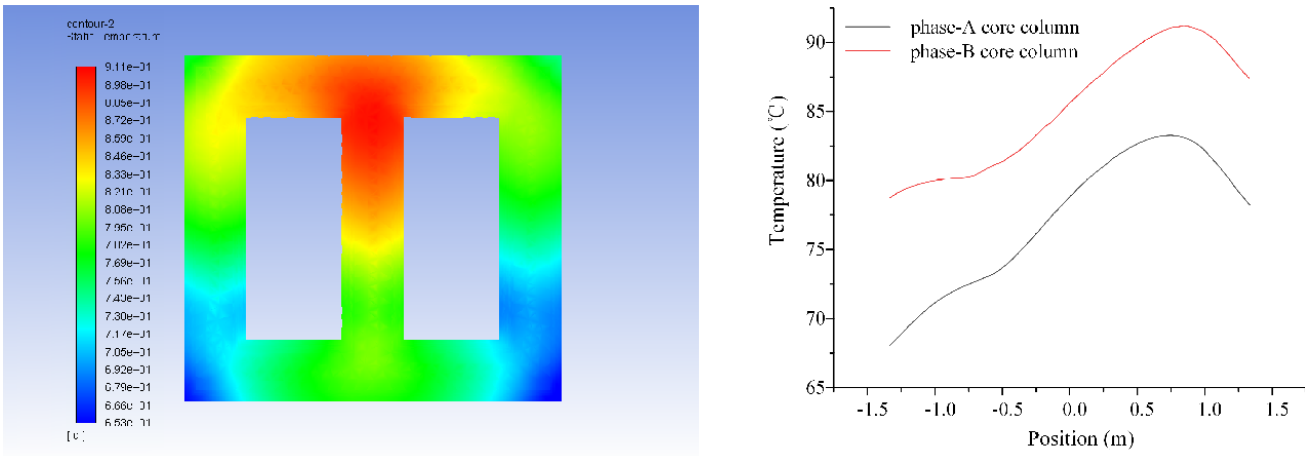

(a) (b)

Figure 8. Temperature field distribution of the core under load.

distribution curve of the core.

It can be seen that the hot spot temperature of core is 91.1°C; the lowest temperature is 65.3°C; and the maximum temperature difference in the core is 25.8°C, which is greater than the maximum temperature difference under no-load condition. Under load, the temperature field distribution of the core is similar to that under no-load condition, that is, the hot spot of the core is located slightly below the upper end of the middle column of the core; the overall temperature distribution tends to gradually decrease from top to bottom; and the temperature at the four corners outside the core is lower. In addition, compared with the temperature field under no-load conditions, the temperatures of phase-A and phase-C core columns increase significantly under load, and the temperature of the phase-B core column showed a significant downward trend from top to bottom. The trend of axial temperature of the core is more obvious according to Figure 8(b). This is because the load loss is greater than the core loss, and the temperature field distribution on the windings affects the temperature field distribution on the core. Figure 9 shows the temperature field distribution on the low-voltage windings. Figure 9(a) shows the temperature field distribution of three phase low-voltage windings, and Figure 9(b) shows the B-phase temperature field distribution of the low-voltage winding. The hot spot on the winding is located near the upper end of the B-phase low-voltage region, and the temperature gradually decreases from top to bottom; therefore, the temperature field distribution characteristics of the core under load exhibit some differences from those under no-load conditions.

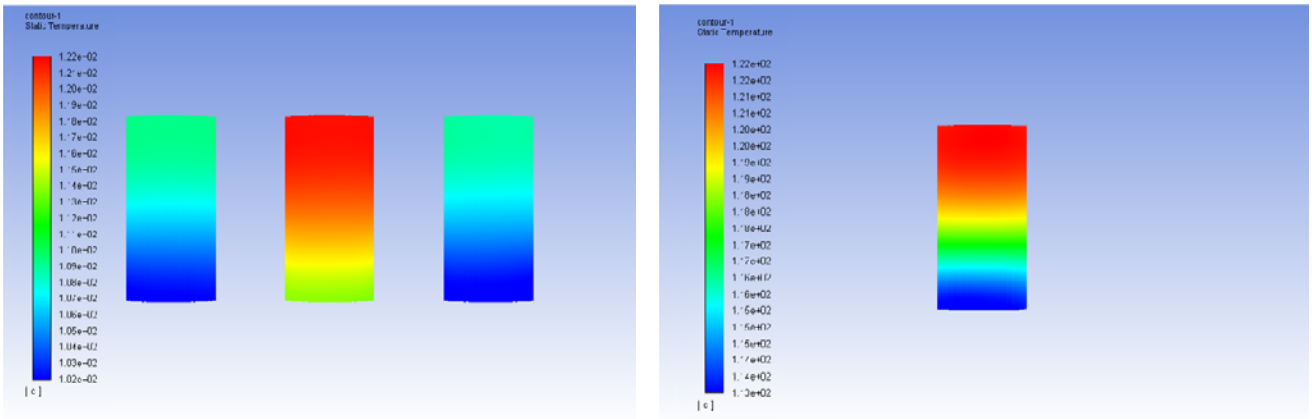

(a) (b)

Figure 9. Temperature field distribution of low voltage windings under load condition.

3.3.3. Analysis of Air Flow Field of the Dry-Type Transformer

Air flow is a key factor affecting the heat dissipation of the transformer, so it is necessary to study the air flow field distribution of the transformer. The vector diagrams of air flow velocity in the $z = 0$ plane and $y = 0$ plane of the transformer under natural air cooling condition are shown in Figure 10 and Figure 11, respectively. It can be seen from the figures that under the condition of natural air cooling, most of the air flows in from the bottom of the tank and flows out from the top. The air flow velocity of the cooling air passage between the transformer windings and the core and the velocity of air flow out of the top of the transformer tank are large.

Natural convection of heat dissipation is usually caused by the difference in density of the air inside the transformer tank. According to the heat transfer theory, there is a heat dissipating air passage inside the dry-type transformer, when the heat of windings and core is transferred from inside to outside surface through heat conduction; the temperature of cooling air in the air passage rises; the volume expands

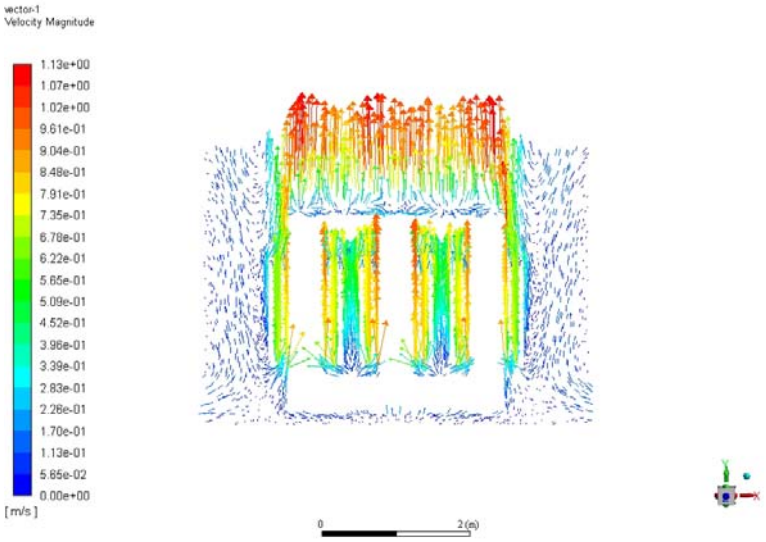

Figure 10. The vector diagram of air flow velocity in the $z = 0$ plane.

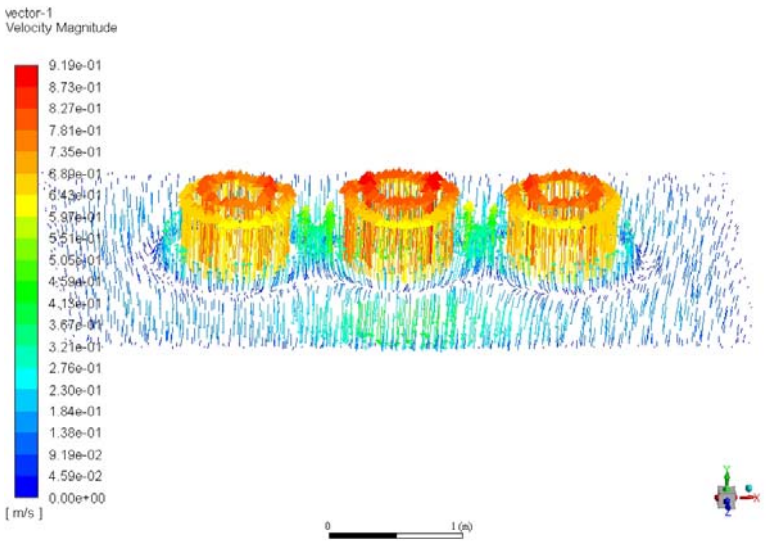

Figure 11. The vector diagram of air flow velocity in the $z = 0$ plane.

and flows upward along the passage. Hot air flows out from the top of the transformer tank, and cold air flows in from the bottom, eventually forming a cycle.

3.3.4. Comparative Analysis with Traditional Average Heat Source Method

The heat source for calculating the temperature field of the core in Section 2 is the loss density distribution obtained from magnetic field analysis, which is imported into the temperature field as the heat source for simulation purposes. This means that the influence of the loss distribution of the core on the temperature distribution is considered. Comparing this method with the traditional method using the average heat source, we superimposed the loss of each unit to obtain the total loss and then divided the total volume to obtain the average amount of heat at source.

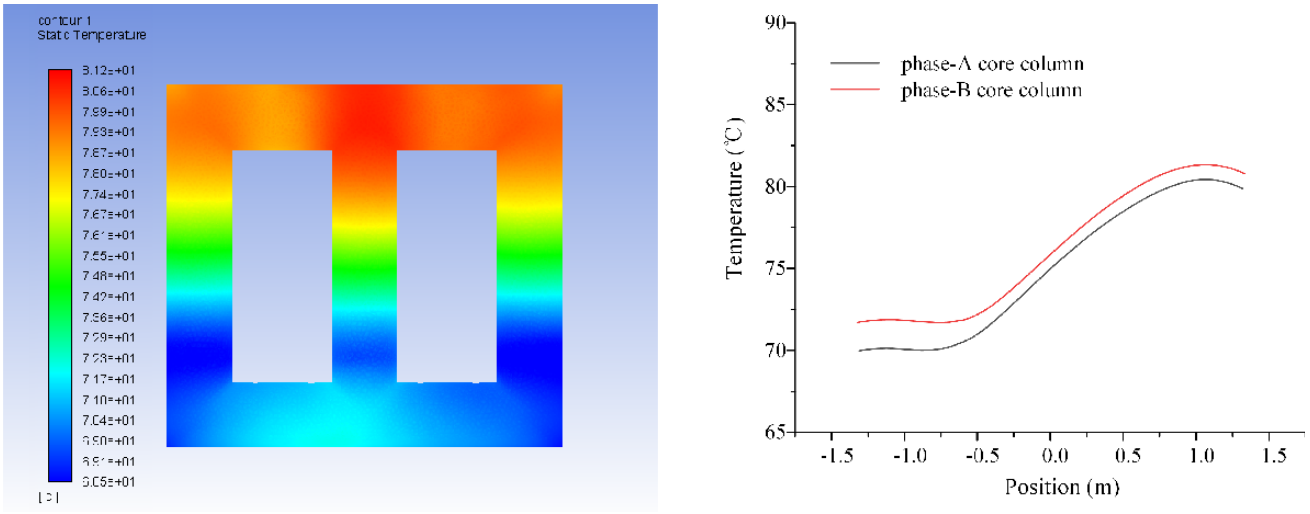

(a) (b)

Figure 12. Temperature field distribution of a dry-type transformer core using the average heat source method.

Figure 12 shows the temperature field distribution of the core under load, as calculated using the average heat source method. Figure 10(a) shows the temperature field distribution nephogram of the core, and Figure 10(b) shows the axial temperature distribution curve of the core. The hot spot temperature of the core is 81.2°C. It can be seen that the temperature distribution characteristics of the core, as simulated by both methods, are similar, including the hot spot position and overall temperature distribution of the core. Different from the non-average heat source used here, the temperature difference between the three-phase core columns is small, and the temperatures of the four corners outside the core are similar to the average temperature. This is because the average heat source method does not consider the core loss density distribution, so the temperature field distribution is mainly affected by the windings: the core temperature field distribution trend is similar to that on the windings.

The deviation using each method is listed in Table 4: the deviation calculated by the proposed method was 2.88%; therefore, the temperature field simulated by the magnetic field loss distribution was closer to the actual transformer core temperature field distribution.

Table 4. Comparison of hot spot temperatures of the core.

Method	Simulated Value	Experimental Value	Deviation
temperature magnetic coupling	91.1°	93.8°	2.88%
average heat source	81.2°		13.43%

4. ANALYSIS OF CORE LOSS AND TEMPERATURE RISE UNDER HARMONIC EXCITATION

4.1. Analysis of Core Loss of a Dry-Type Transformer under Harmonic Excitation

Applying harmonic voltage excitations of different orders and voltage ratio to the transformer, the transient magnetic field analysis of the dry-type transformer allows us to obtain the harmonic core losses under corresponding conditions. The relationship between core loss and harmonic order and harmonic ratio was analyzed.

4.1.1. Analysis of Harmonic Core Loss of a Dry-Type Transformer at Different Harmonic Orders

When the harmonic ratio is 5%, 10%, and 15%, the third, fifth, seventh, ninth, 13th, 17th, and 21st harmonic voltages are applied to the transformer, and the transient magnetic field and core loss under different harmonic orders are obtained. Figure 13 shows the core loss at different harmonic voltage orders.

It can be seen that the relationship between the harmonic core loss and the order of harmonic voltage is that the harmonic loss of the core decreases with the increase of the harmonic order, and the decreasing trend tends to be stable as the order of harmonics increases.

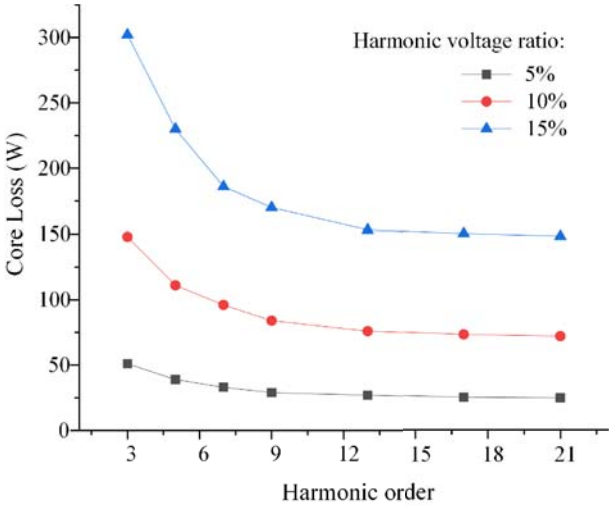

Figure 13. Core loss at different harmonic voltage orders.

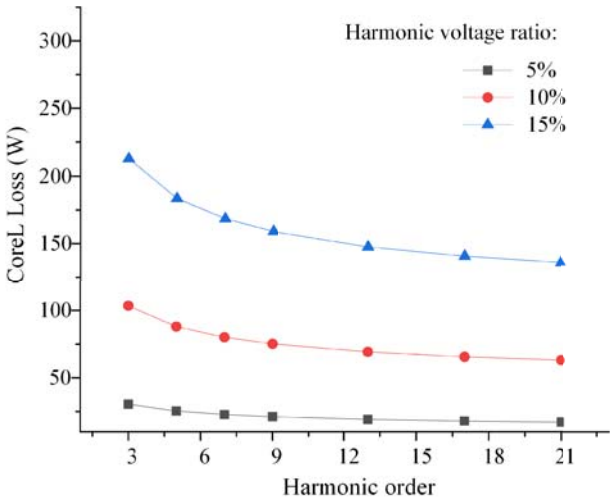

Figure 14. Core loss at different harmonic voltage orders calculated using the empirical formula.

The core loss at different harmonic voltage orders, as calculated by use of the empirical formula (3), is shown in Figure 14. It can be seen by comparing two figures that the simulated value and calculated value change trends are the same, and the results of two methods are similar, thus verifying the accuracy of the simulation.

4.1.2. Analysis of Harmonic Core Loss of a Dry-Type Transformer at Different Harmonic Voltage Ratios

For the 3rd, 5th, 7th, and 9th harmonics, when the harmonic ratio is 3%, 5%, 7%, 10%, 12%, and 15%, the magnetic field of the transformer is simulated to obtain the core loss under corresponding conditions (Figure 13).

It can be seen from Figure 15 that when the harmonic order is constant, the harmonic core loss of the transformer increases with the increase of the harmonic voltage ratio, and the trend is proportional to the square of the harmonic voltage ratio. When the harmonic ratio is less than 3%, the core loss is small and can be ignored.

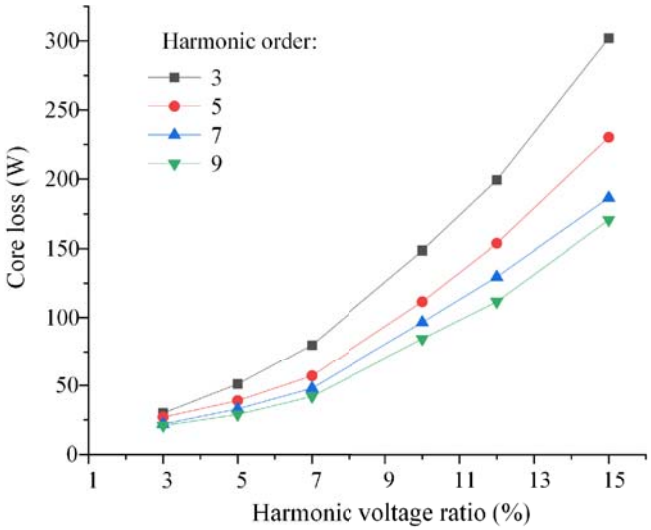

Figure 15. Core loss at different harmonic voltage ratios.

4.2. Analysis of the Temperature Rise in a Dry-Type Transformer Core under Harmonic Excitation

4.2.1. Analysis of the Temperature Rise in the Core at Different Harmonic Orders

The 3rd, 5th, 7th, 9th, 13th, 17th, and 21st harmonics are superimposed on the fundamental voltage (the harmonic content is 5%, 10%, and 15%, respectively), and the magnetic and temperature coupling field is simulated under no-load conditions on a dry-type transformer. The temperature rise in the core at different harmonic orders is shown in Figure 16.

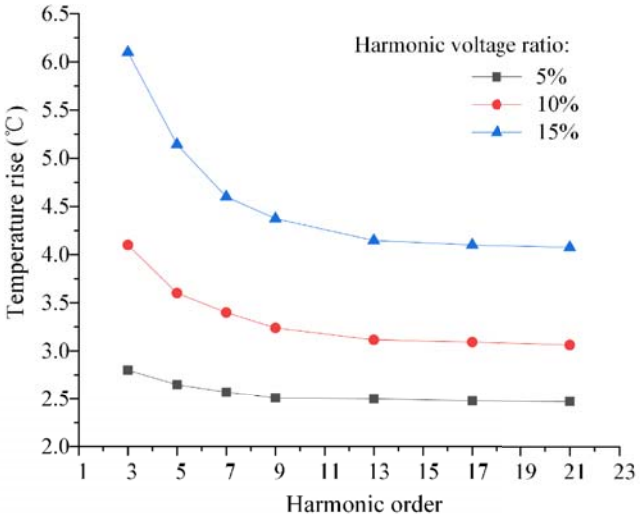

Figure 16. Temperature rise in the core at different harmonic orders.

It can be seen from Figure 16 that the harmonic core loss produces an additional temperature rise in the transformer core, and its temperature rise decreases with the increase of the harmonic order, and gradually becomes smaller. The trend is similar to that in harmonics and core loss. When the order of harmonics is greater than 13, the additional temperature rise generated on the core changes little.

4.2.2. Analysis of the Temperature Rise in the Core at Different Harmonic Voltage Ratios

The harmonic voltages are superimposed on the fundamental voltages at 3%, 5%, 7%, 10%, 12%, and 15%, respectively, at 3rd, 5th, 7th, and 9th harmonics, and the temperature rise in the core at different harmonic ratios, as simulated by the above method, is shown in Figure 17.

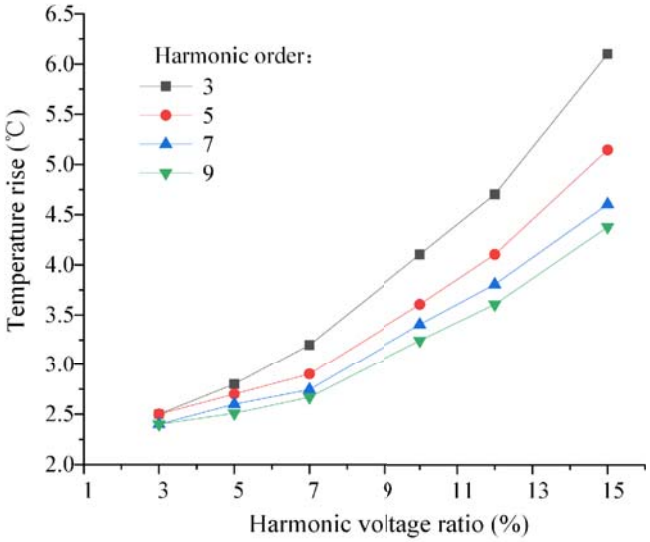

Figure 17. Temperature rise of the core at different harmonic voltage ratios.

Comparing Figure 17 with Figure 15, it can be found that the trend of core loss and core temperature rise are similar under different harmonic voltage ratios, and both increase exponentially with the increase of harmonic voltage ratio. When the harmonic ratio is less than 3%, the temperature rise in the core is negligible; when the harmonic ratio is less than 5%, the temperature rises changes little; when the harmonic ratio is greater than 2.5%, the hot spot temperature on the core changes significantly. If the hot spot temperature of the core is calculated without considering the harmonic no-load loss, the result will be erroneous.

In summary, the harmonics will generate harmonic losses on the dry-type transformer core, which will in turn generate an additional temperature rise. The following results can provide a reference for analyzing the temperature rise in a dry-type transformer core under harmonic excitation.

5. CONCLUSIONS

A magnetic and temperature field coupling analysis method of a dry-type transformer based on FEM was proposed. The core loss and temperature rise of the core were analyzed under different conditions. The results show that the temperature field distribution of the transformer core obtained considering the non-average distribution of core loss density is closer to the actual situation than the average heat source method; in the temperature field analysis, considering air flow could overcome the influence of convective heat transfer analysis and effectively improve the accuracy of temperature field calculation. Therefore, it is necessary to consider the influence of non-average heat source and air flow when calculating the temperature field of the dry-type transformer. According to the temperature field results, the hot spot of the transformer core is located slightly below the upper end of the middle phase core column, which provides a reference for the fixed-point monitoring and life prediction of the dry-type transformer. Core loss and temperature rise of the dry-type transformer under harmonic conditions were analyzed using the proposed method, which could provide a reference for the operation of the dry-type transformer under harmonic conditions.

REFERENCES

1. Rajini, V., "Accurate location of transformer hottest spot by FEM and thermal models," *International Journal of Computer Applications*, Vol. 37, No. 6, 36–41, 2012.
2. Eslamian, M., B. Vahidi, and A. Eslamian, "Thermal analysis of cast-resin dry-type transformers," *Energy Conversion and Management*, Vol. 52, No. 7, 2479–2488, 2011.
3. Wang, S., L. Zhao, K. Lu, et al., "Calculation of transformer loss and insulation life under harmonic currents," *Proceedings of the CSU-EPSA* , Vol. 28, No. 7, 79–88, 2016.
4. Lv, F. and Y. Guo, "Comparative analysis of core loss calculation methods for medium frequency transformer under non-sinusoidal excitation," *High voltage engineering*, Vol. 3, 808–813, 2017.
5. Xu, Y., F. Liu, and Y. Qi, "Prediction of winding temperature in power transformers based on fluid network," *High Voltage Engineering*, Vol. 43, No. 5, 1509–1518, 2017.
6. Zhou, L., H. Tang, L. Wang, et al., "Simulation on three-dimensional temperature field and oil flow field of oil-immersed transformer based on polyhedral mesh," *High Voltage Engineering*, Vol. 44, No. 11, 3524–3531, 2018.
7. Kefalas, T. D. and A. G. Kladas, "Harmonic impact on distribution transformer no-load loss," *IEEE Transactions on Industrial Electronics*, Vol. 57, No. 1, 193–200, 2010.
8. So, E., R. Arseneau, and E. Hanique, "No-load loss measurements of power transformers under distorted supply voltage waveform conditions," *IEEE Transactions on Instrumentation and Measurement*, Vol. 52, No. 2, 429–432, 2003.
9. Tian, M., J. Zhu, J. Song, et al., "Temperature field simulation of coal dry-type transformer based on fluid-solid coupling analysis," *High Voltage Engineering*, Vol. 42, No. 12, 3972–3981, 2016.
10. Feng, Z., L. Zhao, W. Zhou, et al., "Study on temperature rise and load capacity of dry-type transformer under harmonic current," *Proceedings of the CSU-EPSA*, Vol. 29, No. 12, 69–75, 2017.
11. Buccella, C., C. Cecati, and F. de Monte, "A coupled electrothermal model for planar transformer temperature distribution computation," *IEEE Transactions on Industrial Electronics*, Vol. 55, No. 10, 3583–3590, 2008.
12. Liu, G., C. Chi, L. Sun, et al., "Influence of non-uniform temperature on the 2D non-sinusoidal steady AC-DC compound electric field in ±500 kV converter transformer," *Proceedings of the CSEE*, Vol. 38, No. 8, 2521–2562, 2018.
13. Hwang, C. C., P. H. Tang, and Y. H. Jiang, "Thermal analysis of high-frequency transformers using finite elements coupled with temperature rise method," *IEE Proceedings — Electric Power Applications*, Vol. 152, No. 4, 832–836, Aug. 2005.
14. Preis, K., O. Biro, G. Buchgraber, and I. Ticar, "Thermal-electromagnetic coupling in the finite-element simulation of power transformers," *IEEE Transactions on Magnetics*, Vol. 42, No. 4, 999–1002, 2006.
15. Liu, G., Y. Jin, Y. Ma, et al., "Two-dimensional temperature field analysis of oil-immersed transformer based on non-uniformly heat source," *High Voltage Engineering*, Vol. 43, No. 10, 3361–3370, 2017.
16. Tsili, M. A., E. I. Amoiralis, A. G. Kladas, and A. T. Souflaris, "Power transformer thermal analysis by using an advanced coupled 3D heat transfer and fluid flow FEM model," *International Journal of Thermal Sciences*, Vol. 53, 188–201, 2011.
17. Zhang, Y. B., Y. L. Xin, T. Qian, X. Lin, W. H. Tang, and Q. H. Wu, "2-D coupled fluid-thermal analysis of oil-immersed power transformers based on finite element method," *2016 IEEE Innovative Smart Grid Technologies — Asia (ISGT-Asia)*, Melbourne, VIC, 1060–1064, 2016.
18. Zhou, W., D. Wan, H. Ye, et al., "Calculation distribution transformer loss and insulation life assessment under harmonic currents disturbance," *Electrical Measurement & Instrumentation*, Vol. 55, No. 6, 52–58, 2018.